Preparation of Pd-B/γ-Al$_2$O$_3$ amorphous catalyst for the hydrogenation of tricyclopentadiene

Ji-Jun Zou, Zhongqiang Xiong, Li Wang, Xiangwen Zhang [*], Zhentao Mi

Key Laboratory for Green Chemical Technology of Ministry of Education, School of Chemical Engineering and Technology, Tianjin University, Tianjin 300072, PR China

Abstract

Pd-B/γ-Al$_2$O$_3$ amorphous catalysts were prepared through impregnation and KBH$_4$ reduction for the hydrogenation of tricyclopentadiene. The effects of reduction conditions, pre-calcination and thermal annealing on the hydrogenation activity were studied. It is found that the reduction should be conducted in ice water batch with KBH$_4$ solution added by dropping to avoid the crystallization of amorphous metals. Pre-calcination of the catalyst before reduction can increase the amount of Pd on the prepared catalyst. With pre-calcination at 200 °C, the highest hydrogenation turnover frequency is obtained. The amorphous catalyst is thermally stable at temperature below 150 °C. When annealed at higher temperature, the amorphous metals are gradually crystallized and the particle size is increased. After annealing at 600 °C, the catalyst is uniformly crystallized. It is noticed that the size of amorphous Pd calculated from H$_2$-adsorption is much smaller than the actual size observed by transmission electron microscope (TEM). This indicates that amorphous metal has stronger H$_2$-adsorption ability than crystal metals with comparative particle sizes. The hydrogenation activity decreases with the increase of annealing temperature. Moreover, the hydrogenation activity is solely dependent on the amount of H$_2$-adsorption, suggesting that the excellent performance of amorphous catalyst should be attributed to their better H$_2$-adsorption ability.
© 2007 Published by Elsevier B.V.

Keywords: Pd-B/γ-Al$_2$O$_3$; Amorphous catalyst; Tricyclopentadiene; Hydrogenation; Tetrahydrotricyclopentadiene

1. Introduction

High energy density fuel with high density and volumetric energy content (or heating value) can provide more propulsive energy than traditional aviation fuels obtained from refinery [1–5]. Since it can significantly promote the flight distance and loading of aircrafts, the synthesis of high energy density fuel has attracted increasing interests. Generally, these fuels are liquid hydrocarbons with three to five rings. Tetrahydrotricyclopentadiene (THTCPD, tetracyclo [9.2.1.1^{3,9}.0^{4,8}] pentadecane) has been regarded as a potential high energy fuel because of its high density and low viscosity [1–4]. THTCPD is prepared through the hydrogenation of tricyclopentadiene (TCPD, trimer of cyclopentadiene). TCPD has two unsaturated bonds, with one in the norbornene ring and the other in the cyclopentene ring. They are difficult to hydrogenate due to the steric hindrance of tetracyclo-structure. Supported Pt and Pd catalysts can catalyze

the hydrogenation reaction but the activity needs to be improved [1–3]. Therefore, it is necessary to explore more active catalysts.

Amorphous catalysts have attracted much attention because of their superior catalytic activity for the hydrogenation of organics [6–20]. The short-range ordering structures of amorphous catalysts can provide more active and selective sites for hydrogenation reactions. The intensively studied Ni amorphous catalysts exhibit excellent activity for the hydrogenation of many liquid organics [9–16]. However, the amorphous metals are metastable and tend to become crystal particles at high reaction temperature. The presence of nonmetal elements can promote the thermal stability of amorphous metals because of an electron effect. For example, alloy catalysts with B, P, and C elements show good thermal stability [9–16]. Loading of amorphous metals on supports with large surface can also improve the stability and activity because of the interaction between metal and support [14,15]. It has also been shown that pretreatment such as calcination before chemical reduction can enhance the interaction between metal and support, leading to higher activity [16].

Although many amorphous metals have been investigated, the reports on amorphous Pd catalysts are relatively limited. An

---

[*] Corresponding author. Fax: +86 22 27402604.
  E-mail address: zliuying@public.tpt.tj.cn (X. Zhang).

amorphous Pd-B/SiO$_2$ catalyst for nitrobenzene hydrogenation was firstly reported [17]. Then its micro-Raman spectroscopy characterization was reported [18]. Later a Pd-B/γ-Al$_2$O$_3$ amorphous alloy catalyst was prepared for the hydrogenation of anthraquinone [19]. Recently, it is reported that supported noble metals including Pd reduced by glow discharge plasma show some amorphous characteristics [20].

Since Pd-based catalysts are necessary for the hydrogenation of many organics, such as the present case of tricyclopentadiene hydrogenation, Pd-based amorphous catalysts would also find many applications as Ni-based catalysts have done. Previously, we have prepared a Pd-B/γ-Al$_2$O$_3$ amorphous alloy catalyst that exhibits excellent thermal stability [21]. In this work, we prepared this catalyst with different reduction conditions and pre-calcination, estimated the thermal stability, and applied it for the hydrogenation of tricyclopentadiene in liquid phase.

2. Experimental

2.1. Catalyst preparation

Pd-B/γ-Al$_2$O$_3$ amorphous alloy catalyst was prepared by the following procedures. γ-Al$_2$O$_3$ powders (Tianjin Chemical Engineering Design Institute, 100–120 mesh) calcined at 550 °C for 2 h were impregnated with diluted PdCl$_2$ (Xian Kaili Chemical Engineering Company) solution. The initial amount of Pd was defined as 0.4 wt.% for all the experiments. After dried at 120 °C for 2 h, the catalysts were pre-calcined at defined temperature for another 2 h. Then they were reduced by adding KBH$_4$ solution (0.2 M) under gentle stirring in an ice water bath for about 30 min until no obvious bubbles were observed. The resulting black solid powders were washed thoroughly with oxygen-free distilled water until no Cl$^-$ ions were detected in the solution and subsequently with pure alcohol. Thermal annealing was carried out in N$_2$ atmosphere at defined temperature for 2 h. For X-ray diffractive (XRD) characterization, MCM-41 (Tianda Beiyang Company) was used as the support to avoid the diffraction peaks of Pd being overlapped by those of support. For the purpose of comparison, traditional 0.4 wt.% Pd/γ-Al$_2$O$_3$ catalyst was prepared by routine impregnation followed with H$_2$ reduction at 300 °C for 2 h.

2.2. Catalyst characterization

The chemical status of prepared Pd was analyzed using X-ray photoelectron spectroscopy (XPS, Perkin-Elmer PHI-1600) with Al Kα radiation (1486.6 eV). The binding energy was calibrated using the C$_{1s}$ peak (284.6 eV) of contaminant carbon. The crystal structure of prepared metals was characterized using XRD (D/MAX-2500, Cu Kα radiation). The amount of Pd supported on the catalysts was determined using inductively coupled plasma spectrometry (ICP-OES, Vista-MPX). The metal particles were observed with transmission electron microscope (TEM, Tecnai G^2 F-20, Philips) equipped with energy-dispersive X-ray (EDX) instrument. The specific surface area was measured using N$_2$ physical adsorption (Quantachrome Nova-2000) with a multi-plot method. The H$_2$-adsorption was conducted at 29 °C with an Auto Chem 2910 analyzer (Micrimetritice).

2.3. Activity evaluation

TCPD used for the hydrogenation reaction was prepared by the oligomeraiztion of cyclopentadiene and then distillation to remove the un-reacted feedstock according to previous work [4]. The purity of obtained TCPD was >96% as determined by GC. The hydrogenation reaction of TCPD was carried out in a 250 mL mechanically agitated reactor containing 150 mL TCPD in cyclohexane (0.16 M) and 0.45 g catalyst. The reactor was purged with N$_2$ to eliminate oxygen and then filled with H$_2$ and heated to 110 °C. This low hydrogenation temperature was chosen to avoid the decomposition or oligomerization of thermally unstable TCPD. The hydrogenation reaction was started with vigorous stirring (1000 rpm). The H$_2$ pressure (1.5 MPa) was maintained at constant value by continuously supplying the consumed gas. The reaction was carried out for 4 h. Then the reaction mixture was cooled to room temperature by flowing water. The obtained products were analyzed with HP-5971 GC–MS equipped with HP-5 capillary column (0.53 mm × 30 m). Their concentrations were analyzed using a GC (HP 4890, FID) equipped with the same HP-5 capillary column and determined through the area normalization method.

3. Results and discussion

3.1. Hydrogenated products

GC–MS analysis shows that the hydrogenated products include dihydrotricyclopentadiene (DHTCPD) with the bond in norbornene ring saturated and completely saturated tetrahydrotricyclopentadiene. Fig. 1 shows that the concentration of reactant and products vary with the reaction time. The concen-
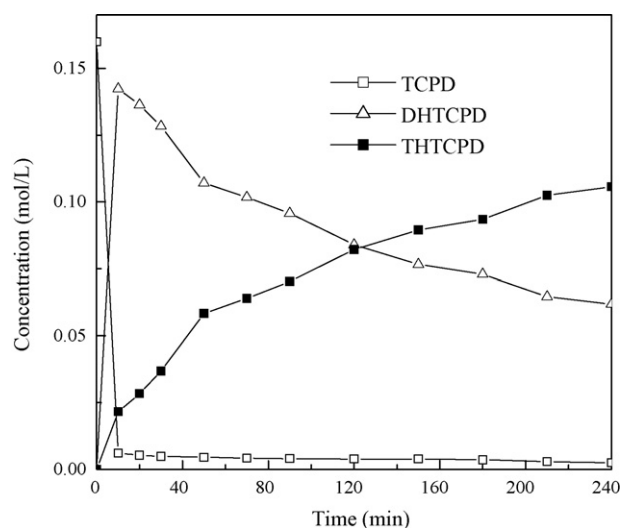

Fig. 1. Concentration of reactant (TCPD), hydrogenated intermediate (DHTCPD) and product (THTCPD) involving with reaction time.
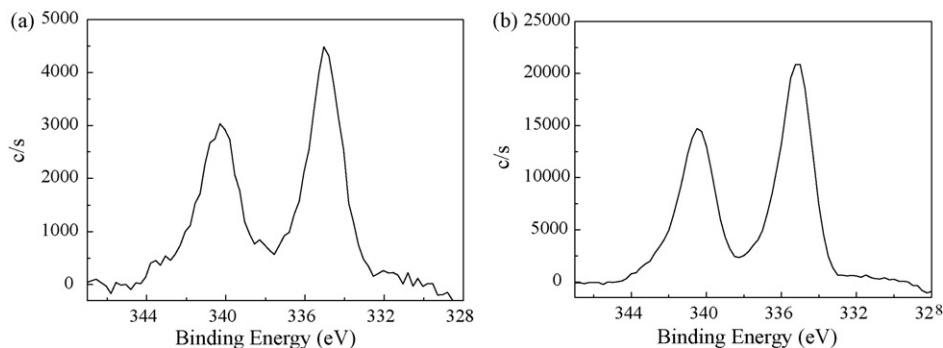
Fig. 2. Pd XPS spectra of (a) Cat-I and (b) Cat-II. (The catalysts were pre-calcined at 300 °C for 2 h before KBH_4 reduction.)

tration of TCPD decreases quickly and a conversion of more than 95% is obtained within 10 min. Correspondingly, the concentration of DHTCPD reaches a highest value during this period and begins to decline after that. The concentration of THTCPD always increases with the increase of reaction time. This tendency is a characteristic of consecutive reaction. Thus, the hydrogenation of TCPD takes place according to the following steps:
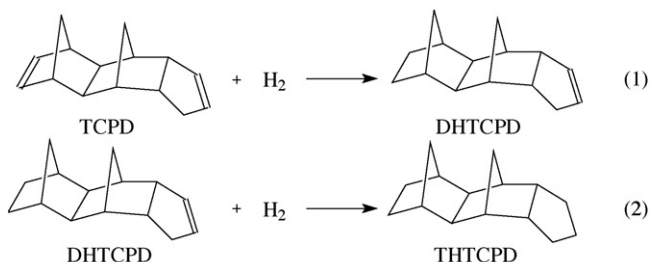
The first step is easy to take place and different catalysts show similar activity. However, the second step is difficult to occur and different catalysts exhibit different activity. Therefore, the yield of THTCPD obtained from the second step is used to assess the hydrogenation activity of different catalysts.

3.2. Effect of reduction conditions

The reduction conditions were studied to find an optimal reduction operation. KBH_4 solution was added by slow dropping (0.5 mL/min) or quick pouring, and the resulting catalyst was denoted as Cat-I and Cat-II, respectively. XPS analysis in Fig. 2 shows that the Pd spectra contain two peaks with binding energy at 335.0 and 340.1 eV. These two peaks are assigned to the electron transitions of $3d_{5/2}$ and $3d_{3/2}$ of Pd^0, which indicates that in both cases the Pd^{2+} can be reduced to metallic Pd^0. However, XRD characterization in Fig. 3 shows that the Pd particles reduced by two methods have different crystal structure. For Cat-I, Pd shows only a broad peak at $2\theta = 40°$ that is the characteristic of amorphous Pd [16]. Nevertheless, Cat-II has three strong peaks at $2\theta = 40°$, 46° and 68°. These peaks are assigned to (1 1 1), (2 0 0) and (2 2 0) face of cubic crystal Pd. This suggests that some amorphous metals have become crystals. Moreover, during this reduction operation, a temperature rise of 10 °C in the suspension of catalyst powders is observed. When KBH_4 solution is quickly poured into the catalyst, the reduction reaction is so violent that the heat is quickly accumu-

lated. In this case, hot spots may be formed on catalyst surface, resulting in the crystallization of amorphous Pd.

The result mentioned above indicates that the reduction temperature may be an important factor influencing the crystal structure of catalyst. So a third reduction operation was conducted and the resulting catalyst was denoted as Cat-III. The reduction conditions are similar to Cat-I but a 15 °C water bath was used to replace ice water bath. The XRD patterns of Cat-III are also shown in Fig. 3. It is obvious that there are three diffraction peaks at $2\theta = 40°$, 46° and 68°, indicating the formation of Pd crystals. According to the intensity of diffraction peaks, the crystallinity of the three samples is as following: Cat-III > Cat-II > Cat-I. Therefore, the reduction temperature has to be carefully controlled in order to obtain amorphous Pd catalyst.

The activity of the three catalysts was evaluated for the hydrogenation of TCPD. Since they have different crystallinity, the data may reflect the effect of crystallinity on the hydrogenation activity. The yield of THTCPD on the three catalysts is as following: Cat-I(73.5%) > Cat-II(71.2%) > Cat-III(69.9%). It is clear that amorphous Pd catalyst shows higher activity than the crystal Pd catalyst. In the following sections, all the reduction operations were conducted
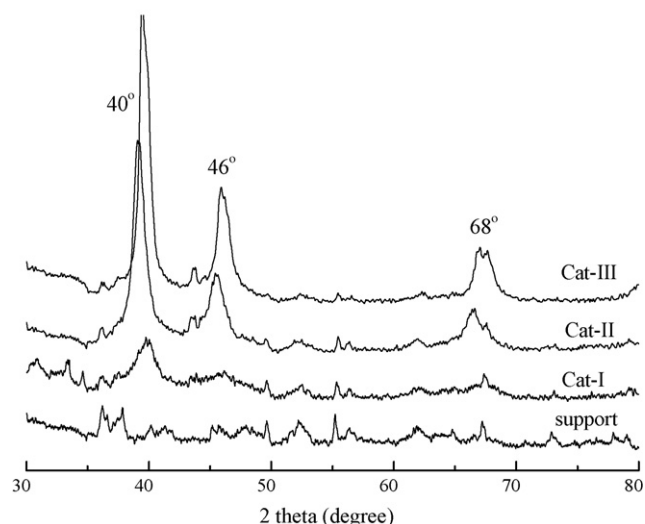

Fig. 3. XRD patterns of Cat-I, Cat-II and Cat-III. (The catalysts were pre-calcined at 300 °C for 2 h before KBH_4 reduction.)
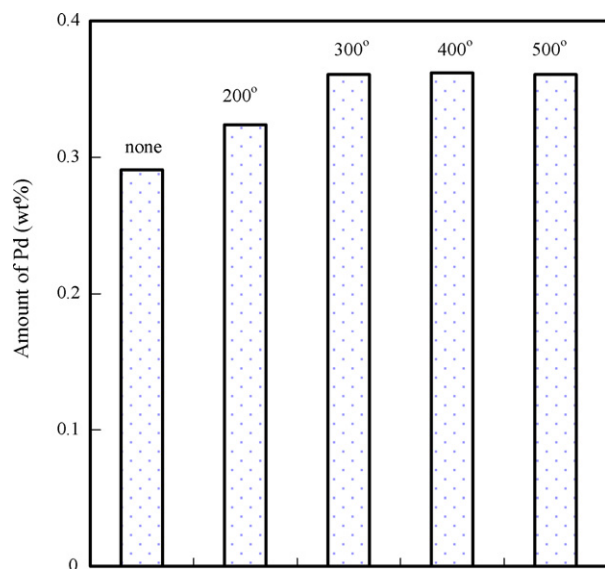
Fig. 4. Amount of Pd on Pd-B/γ-Al$_2$O$_3$ catalysts prepared with pre-calcination at different temperature.
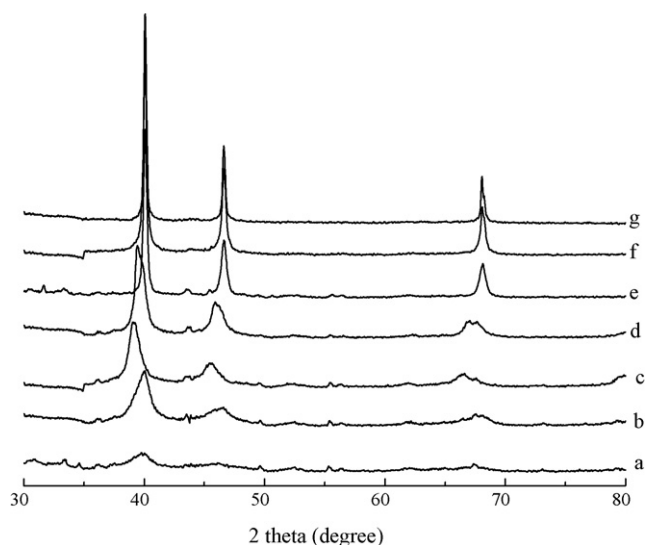

Fig. 5. XRD patterns of (a) fresh amorphous catalyst, (b) annealed at 150 °C, (c) annealed at 300 °C, (d) annealed at 450 °C, (e) annealed at 600 °C, (f) annealed at 800 °C, and (g) H$_2$-reduced catalyst.

in ice water batch with KBH$_4$ solution added by slow dropping.

3.3. Effect of pre-calcination

In this section, the catalysts were pre-calcined at different temperature before KBH$_4$ reduction. ICP analysis in Fig. 4 shows that this pretreatment can increase the amount of Pd on the prepared Pd-B/γ-Al$_2$O$_3$ catalyst. For the catalyst without pre-calcination, the amount of Pd is only 0.291 wt.%, which is dramatically lower than the initial defined amount of 0.4 wt.%. This means that the interaction between impregnated Pd^{2+} ions and support is not strong enough to anchor Pd particles on the support surface. Pre-calcinations at proper temperature can enhance the interaction between Pd^{2+} ions and support, and thus, stably anchor the metal particles on the support surface. The amount of Pd is increased to 0.361 wt.% after pre-calcination at 300 °C, but higher pre-calcination temperature does not improve the effect any more.

Table 1 shows the activity of catalysts with pre-calcination at different temperature. The catalyst without pre-calcination leads to a yield of THTCPD as 60.6%, whereas those with pre-calcination exhibit a yield above 73.0%. Therefore, the pre-calcination can significantly improve the hydrogenation activity. This is reasonable because pre-calcination can increase the amount of Pd on the resulting catalyst. To evaluate the

activity of per Pd atom, the turnover frequency (TOF) of Pd atoms was calculated as shown in Table 1. It is found that pre-calcination at 200 °C leads to a highest TOF value, indicating that the interaction between metal and support can enhance the hydrogenation activity of amorphous Pd. Nevertheless, pre-calcination at higher temperature conversely results in lower TOF value, suggesting that too strong interaction between metal and support may suppress the hydrogenation activity. To obtain a high overall hydrogenation yield, in the following sections, all the catalysts were pre-calcined at 300 °C for 2 h before KBH$_4$ reduction.

3.4. Thermal stability and effect of annealing

To evaluate the thermal stability of amorphous catalysts, the catalysts were annealed at defined temperature for 2 h. Fig. 5 shows the XRD patterns of annealed and H$_2$-reduced catalysts. The fresh sample shows a typical amorphous characteristic with a weak and broad peak at $2\theta = 40°$. There is no obvious change in the XRD patterns when the annealing temperature is below 150 °C, indicating that the amorphous structure is thermally stable under this temperature. With the annealing temperature rising, the diffraction peak gradually grows and a new peak at $2\theta = 46°$ appears, which means the occurrence of crystallization process. When the temperature reaches 600 °C, a sharp peak at $2\theta = 68°$ is observed. The diffraction peaks do not change any

Table 1
Hydrogenation activity of fresh Pd-B/γ-Al$_2$O$_3$ catalysts with different pre-calcination temperature

Pre-calcination temperature (°C)	Conversion of TCPD (%)	Selectivity of THTCPD (%)	Yield of THTCPD (%)	TOF (s^{-1})
0	97.3	62.3	60.6	8.3
200	97.0	73.6	71.4	8.9
300	96.9	75.8	73.5	8.2
400	96.9	75.1	72.8	8.1
500	96.5	76.7	74.0	8.2

Table 2
Surface area, H$_2$-adsorption and activity of Pd-B/γ-Al$_2$O$_3$ catalysts with different annealing temperature

Annealing temperature (°C)	Pd-B/γ-Al$_2$O$_3$					H$_2$-reduced Pd/γ-Al$_2$O$_3$
	Fresh	150	300	450	600	
BET (m^2/g$_{Cat}$)	190.2	191.0	186.8	179.4	177.1	180.3
H$_2$-adsorption (μmol/g$_{Cat}$)	9.77	8.21	7.54	6.83	6.65	6.69
Calculated metal size (nm)	1.6	3.0	3.5	7.8	11.9	10.3
Yield of THTCPD (%)	73.5	70.1	67.6	64.9	64.5	65.1

more at higher annealing temperature because the amorphous catalyst has been uniformly crystallized. In fact, the catalysts annealed at 600 and 800 °C show very similar patterns to the traditional H$_2$-reduced sample.

To monitor the crystallization process in more detail, the in-situ annealing was characterized using XRD. The sample was heated from 50 to 600 °C in N$_2$ and the data were recorded at 50 °C interval. The crystallinity at different temperature were calculated using the intensities of the (1 1 1), (2 0 0) and (2 2 0) peaks with those of H$_2$-reduced sample as reference:

Crystallinity (%)

$$= \frac{[I(1\,1\,1) + I(2\,0\,0) + I(2\,2\,0)]_{sample}}{[I(1\,1\,1) + I(2\,0\,0) + I(2\,2\,0)]_{H_2\text{-reduced}}} \times 100\%$$

As shown in Fig. 6, the crystallinity is zero at temperature below 150 °C and relatively low at temperature below 200 °C. It gradually rises up with the increase of annealing temperature and reaches 100% to 600 °C. Therefore, it is expected that the amorphous catalyst could be used at temperature below 200 °C without obvious change in amorphous structure.

Fig. 7 shows the TEM images of fresh and annealed Pd-B/γ-Al$_2$O$_3$ catalysts. Metal particles on fresh catalyst are not obvious because they are homogeneously dispersed on the support. EDX analysis detects both Pd and B elements, confirming the existence of Pd-B alloys on the catalyst particles. The size of metal particles increases to about 5 nm after annealing at 150 °C, indicating the aggregation and growth of Pd particles during annealing treatment. This aggregation is more serious at
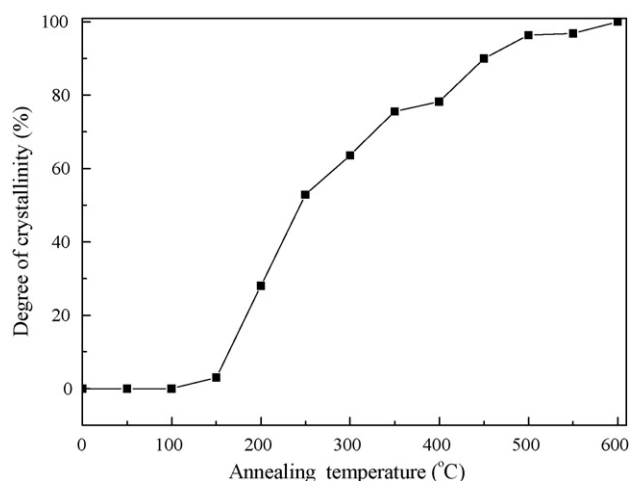
higher annealing temperature. The particle size is bigger than 10 nm when the annealing temperature is above 450 °C but does not change much when the annealing temperature is further increased.

Table 2 shows the result of physical and chemical adsorptions of fresh and annealed Pd-B/γ-Al$_2$O$_3$ catalysts. The BET surface of fresh catalyst is 190.2 m^2/g, which is slightly decreased after annealing due to the aggregation in Pd particles. The amount of H$_2$-adsorption also decreases with the increasing of annealing temperature. Since H$_2$-chemisorption has been widely used to calculate the particle size of supported metals, the particle size of fresh and annealed catalysts was calculated in this work. The particle size of thoroughly crystallized catalysts, i.e. Pd-B/γ-Al$_2$O$_3$ annealed at 600 °C and Pd/γ-Al$_2$O$_3$ reduced by H$_2$ at 300 °C, is in agreement with the results observed by TEM. However, for amorphous catalysts, the size derived from H$_2$-adsorption is dramatically smaller than the actual size observed by TEM. This result suggests that the amorphous metals can adsorb more H$_2$ than the crystal metals with comparative particle size (or surface area). Furthermore, this strong H$_2$-adsorption ability of amorphous catalyst may be a reason for their excellent hydrogenation performance.

The activities of fresh and annealed Pd-B/γ-Al$_2$O$_3$ catalysts are shown in Table 2. The yield of THTCPD is 73.5% for the fresh catalyst. It gradually decreases to 64.5% when the catalyst is annealed in the temperatures range of 150–600 °C. This indicates that annealing has a negative effect on the activity of catalysts. It can be explained by the two factors. First, the crystallized metals show a lower activity than amorphous metals. Second, the growth of metal particle reduces the active sites on the metal surface. For Pd-B/γ-Al$_2$O$_3$ annealed at 150 °C, the lower activity compared with the fresh catalyst is due to the growth of metal particles because they have similar amorphous structure. Pd-B/γ-Al$_2$O$_3$ annealed at 600 °C shows activity similar to the H$_2$-reduced catalyst because they have identical crystallinity and particle size.

It is worthy to note that the hydrogenation activity can also be assessed in terms of H$_2$-adsorption. Fig. 8 shows the correlation between the yield of THTCPD and the amount of H$_2$-adsorption of six catalysts involved in Table 2. The hydrogenation activity monotonously increases with the increase in H$_2$-adsorption, and a good linear relationship is obtained. It is evident that the hydrogenation activity is solely dependent on the H$_2$-adsorption ability of catalysts. It also suggests that the high hydrogenation activity of amorphous Pd should be attributed to its strong H$_2$-adsorption capacity.
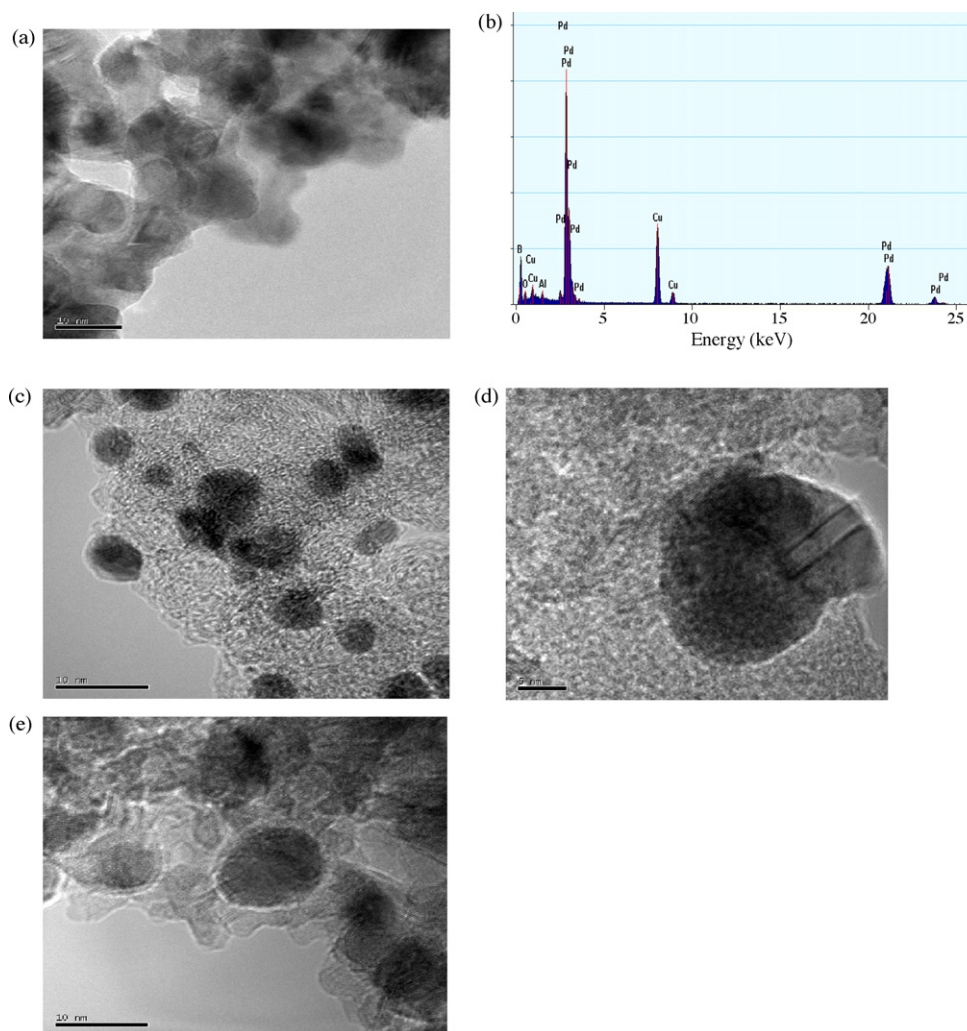

Fig. 6. Crystallinity of catalyst dependent on the annealing temperature.

Fig. 7. TEM images of (a) fresh Pd-B/γ-Al$_2$O$_3$, (b) its EDX analysis, (c) annealed at 150 °C, (d) annealed at 450 °C and (e) annealed at 600 °C.

4. Conclusion

We have prepared Pd-B/γ-Al$_2$O$_3$ amorphous catalysts using impregnation followed by KBH$_4$ reduction and applied them for the hydrogenation of TCPD to THTCPD. The reduction should be conducted in ice water batch and KBH$_4$ solution should be added with slow dropping to avoid the crystallization of amorphous Pd. Pre-calcination before KBH$_4$ reduction can enhance the interaction between the metal and support, increase the amount of Pd on the catalyst and improve the hydrogenation activity. The amorphous catalyst is very stable at temperature below 150 °C. Annealing at higher temperature leads to the crystallization and growth of amorphous metals. Amorphous metals show stronger H$_2$-adsorption ability and hydrogenation activity than crystal metals with comparative particle size. The hydrogenation activity of Pd catalyst is linearly dependent on the amount of H$_2$-adsorption.
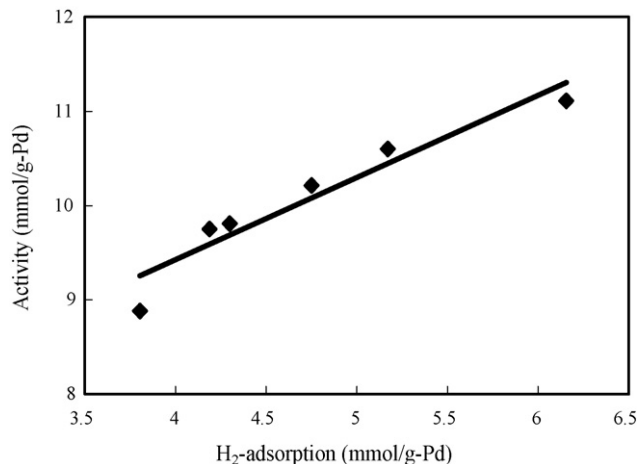
Acknowledgements

Fig. 8. Relationship between hydrogenation activity and H$_2$-adsorption capacity of Pd-based catalysts.

References

[1] H.S. Chung, C.S.H. Chen, R.A. Kremer, J.R. Boulton, Energ. Fuel. 13 (1999) 641–649.

[2] W.B. George, A.I. Schneider, U.S. Patent 4,401,837 (1983).

[3] R.B. James, A.I. Schneider, U.S. Patent 5,446,222 (1995).

[4] Z. Xiong, Z. Mi, X. Zhang, React. Kinet. Catal. Lett. 85 (2005) 89–97.

[5] E. Xing, Z. Mi, C. Xin, L. Wang, X. Zhang, J. Mol. Catal. A: Chem. 231 (2005) 161–167.

[6] J.-F. Deng, H. Li, W. Wang, Catal. Today 51 (1999) 113–125.

[7] J.A. Schwarz, C. Contescu, A. Contescu, Chem. Rev. 95 (1995) 477–510.

[8] S. Liu, Z. Liu, Z. Wang, S. Zhao, Y. Wu, Appl. Catal. A: Gen. 313 (2006) 49–57.

[9] S. Ge, Z. Wu, M. Zhang, W. Li, K. Tao, Ind. Eng. Chem. Res. 45 (2006) 2229–2234.

[10] H. Li, H. Luo, L. Zhang, W. Dai, M. Qiao, J. Mol. Catal. A: Chem. 203 (2003) 267–275.

[11] L.-F. Chen, Y.-W. Chen, Ind. Eng. Chem. Res. 45 (2006) 8866–8873.

[12] Z. Jiang, H. Yang, Z. Wei, Z. Xie, W. Zhong, S. Wei, Appl. Catal. A: Gen. 279 (2005) 165–171.

[13] X. Yan, J. Sun, Y. Wang, J. Yang, J. Mol. Catal. A: Chem. 252 (2006) 17–22.

[14] Y.-Z. Chen, B.-J. Liaw, S.-J. Chiang, Appl. Catal. A: Gen. 284 (2005) 97–104.

[15] H. Li, W. Wang, H. Li, J.-F. Deng, J. Catal. 194 (2000) 211–221.

[16] H. Li, H. Li, W.-L. Dai, J.-F. Deng, Appl. Catal. A: Gen. 207 (2001) 151–157.

[17] X. Yu, M. Wang, H. Li, Appl. Catal. A: Gen. 202 (2000) 17–22.

[18] G. Wang, X. Yu, X. Cao, H. Li, Z. Zhang, J. Raman Spectrosc. 31 (2000) 1051–1055.

[19] T. Ding, Y.N. Qin, Z. Ma, Chin. Chem. Lett. 14 (2003) 319–322.

[20] J.-J. Zou, Y.-P. Zhang, C.-J. Liu, Langmuir 22 (2006) 11388–11394.

[21] Z. Xiong, Z. Mi, X. Zhang, Catal. Commun. 8 (2007) 571–575.